PERGAMON

International Journal of Solids and Structures 39 (2002) 5515–5528

INTERNATIONAL JOURNAL OF SOLIDS and STRUCTURES

www.elsevier.com/locate/ijsolstr

On transient ultrasonic waves in a homogeneous plate with thin superconducting coating layers

A. Jonas Niklasson [a,*], Subhendu K. Datta [b]

[a] *Department of Applied Mechanics, Chalmers University of Technology, SE-412 96 Göteborg, Sweden*
[b] *Department of Mechanical Engineering, University of Colorado, Boulder, CO 80309-0427, USA*

Received 9 October 2001; received in revised form 5 March 2002

Abstract

Transient guided waves excited by a line force applied on one surface of a plate with thin superconducting anisotropic layers deposited symmetrically on both surfaces of a core metallic material are considered here. The line of force is assumed to make an arbitrary angle to an axis of symmetry of the anisotropic layer. Thus, the displacement at any point in the plate has all the three components but it is independent of the coordinate parallel to the line force (taken as x_2-axis). Attention is focused here on the coupling of the longitudinal and flexural motion with the horizontally polarized shear motion. It is shown that this coupling causes an interchange between longitudinal (or flexural) and shear horizontal modes at certain frequencies, which are not high. As a result, when the center frequency of a narrow band excitation is near one of the strong coupling frequencies the received signal has characteristic features that are quite different than for other frequencies. These features could be used to characterize in-plane anisotropy of the thin layers using transducers operating at moderate frequencies.

Keywords: Ultrasonic guided waves; Elastic wave propagation; Transient waves; Thin superconducting coatings

1. Introduction

In this paper, our attention is focused on the transient response of a plate composed of *thin* anisotropic superconducting layers deposited on a homogeneous metallic plate. For simplicity, the problem considered is the case when the thin layers are of uniform thickness h and are deposited symmetrically on both surfaces of the homogeneous core plate. The analysis is easily extended to the case when the coating layer is only on one surface. The motivation is to develop a fundamental understanding of ultrasonic guided waves in tapes that are fabricated for commercial high-current applications. These tapes are composites consisting of a brittle superconducting phase and a ductile metal phase. Various mechanical processes are used to get the crystallographic texture most favorable to high-current capacity of the tapes. Such processes coupled with

* Corresponding author. Fax: +46-31-772-3827.
E-mail address: jonas.niklasson@me.chalmers.se (A.J. Niklasson).

0020-7683/02/$ - see front matter
PII: S0020-7683(02)00362-1

thermal cycling cause microcracking of the brittle oxide layers, which limit the current carrying capacity. The degree of current capacity reduction is a strong function of the crystallographic texture of the oxide layer and the extent of microcracking, which is also a function of texture. These effects influence the mechanical response such as ultrasonic guided waves along the tapes. So, the ultrasonic guided waves provide an efficient means to determine in situ elastic anisotropic constants of the layer and thus, can be used for material property characterization during and after processing of the tapes.

There is a large body of literature on ultrasonics in superconducting bulk materials. It is now well established that the elastic constants are linked to the superconducting transition temperature T_C through the Debye temperature Θ_D and the electron–phonon coupling parameter λ (Lei et al., 1993; Shindo et al., 1995). A review of various ultrasonic measurements of elastic properties can be found in Levy (1993). Investigation of the in situ mechanical behavior and properties of thin superconducting layers has been limited. Since the properties are highly dependent upon external and internal stress fields, interface properties and porosity, to name a few, it is necessary to understand the basic problem of guided ultrasonic wave propagation in a three-layered tape.

Pan and Datta (1999) studied the dispersion of waves propagating in a direction of material symmetry of the orthotropic $YBa_2Cu_3O_{7-\delta}$ (YBCO) layer(s) in three-layered (YBCO/Ni/YBCO and Ni/YBCO/Ni) tapes. They also studied the transient response of such a plate due to the application of a line force orthogonal to the symmetry axis and acting perpendicular to the plate surface. In the present study, the analysis is extended to include propagation in an arbitrary planar direction. Our recent studies (Niklasson et al., 2000a,b) on dispersion of ultrasonic guided waves in the presence of anisotropic coating or interface layers have shown that because of anisotropy extensional (S) and flexural (A) modes become coupled with the shear horizontal (SH) for propagation in arbitrary planar directions. They are uncoupled when propagation is along an axis of symmetry, as discussed by Pan and Datta (1999). Thus, for off-symmetry-axis propagation in-plane elastic constants C'_{12} and C'_{66} (see Fig. 1 for the definition of the Cartesian coordinate axes x_1, x_2, and x_3), which do not influence S and A motion along the symmetry axes, cause considerable modification of the modes. Here, prime denotes elastic constants referred to the symmetry axes. It is found that strong coupling occurs at relatively low frequencies, at which interchanges of modes take place. Measurements at frequencies centered around these strong coupling frequencies would then allow determination of these in-plane constants. In recent years, most investigations of thin layer anisotropic elastic constants have been carried out at very high frequencies (~GHz) using acoustic microscopy (Kim et al., 1992; also see Qu and Kundu, 2000). In this paper, we present a model study of transient wave propagation in a symmetrically layered YBCO/Ni/YBCO plate excited by a line force applied normally to one surface of the plate. The attention is focused on the region of excitation frequency where the S_0 and SH_0 modes are strongly coupled (~25–40 MHz) and they interchange energy at around 32 MHz for the

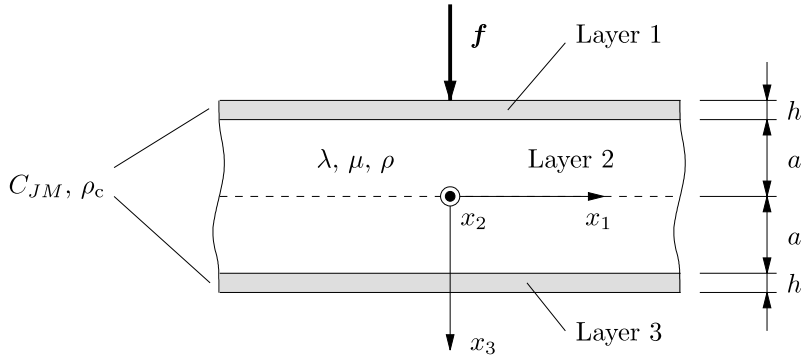

Fig. 1. A line force on a coated plate.

particular case considered here. At 32 MHz, the thickness of the YBCO coating layers is roughly 5% of the wavelength of the S_0 and SH_0 modes making this frequency relatively low. In an earlier paper, Niklasson and Datta (submitted for publication) presented a detailed analysis of transient waves in a plate composed of a thin YBCO layer sandwiched between two isotropic homogeneous nickel layers. The case of an YBCO coated Ni plate was also discussed briefly in the above mentioned paper. That analysis is presented in much greater detail in the present paper. In Niklasson and Datta (submitted for publication), approximate equations appropriate for thin interface and coating layers were presented also. So, the details will be omitted in this paper. Only a brief summary is presented in Section 4.

Numerical results were obtained using both an exact modeling applicable to multilayered anisotropic plates and the approximation for thin layers deposited on a plate. Both show good agreement at moderate frequencies. However, the approximation shows a systematic error at high frequencies.

2. Problem statement

The configuration studied in this paper is depicted in Fig. 1. An infinite, isotropic, homogeneous plate (layer 2) of thickness $2a$ is coated symmetrically with two thin superconducting (anisotropic) layers (layers 1 and 3), each of thickness h. It is assumed that the thickness of the coating layers, h, is small compared to the wavelengths (this assumption is actually only needed in Section 4). On the top surface of the coated plate, at $x_1 = 0$ and $x_3 = -a - h$, a line force $\mathbf{f}$, parallel to the x_2-axis, is applied. In the figure, a line force acting in the x_3-direction is shown. Due to the line force, all fields will be independent of x_2. The aim of this paper is to study the transient response due to the line force on the same surface as the force is applied, i.e., at a point $x_1 = \xi$, $x_3 = -a - h$.

The relevant material parameters of the isotropic, homogeneous plate are the Lamé constants λ and μ and the density $\rho^{(2)} = \rho$. The superconducting coating layers are assumed to be anisotropic with the x_1x_2-plane as a plane of elastic symmetry, i.e., monoclinic material symmetry. The material parameters of interest to elastic wave propagation are the elastic constants C_{JM} and the density $\rho^{(1)} = \rho^{(3)} = \rho_c$.

It is assumed that all fields have been temporally Fourier transformed. Temporally Fourier transformed functions are denoted by uppercase letters, for example,

$$G(\omega) = \int_{-\infty}^{\infty} g(t)\mathrm{e}^{\mathrm{i}\omega t}\,\mathrm{d}t, \Rightarrow g(t) = \frac{1}{2\pi}\int_{-\infty}^{\infty} G(\omega)\mathrm{e}^{-\mathrm{i}\omega t}\,\mathrm{d}\omega, \tag{2.1}$$

where t is time, ω is the circular frequency and $\mathrm{i} = \sqrt{-1}$. In each layer $r = 1, 2, 3$, the elastodynamic equations of motion,

$$\partial_\alpha \Sigma^{(r)}_{\alpha j} + \rho^{(r)}\omega^2 U^{(r)}_j = 0, \tag{2.2}$$

hold, where $U^{(r)}_j$ is the displacement vector, $\Sigma^{(r)}_{jm}$ is the stress tensor, and ∂_j means $\partial/\partial x_j$. The lowercase Roman indices run over 1, 2 and, 3, the lowercase Greek indices run over 1 and 3, and the summation convention is employed. The constitutive equations for the isotropic plate are given by

$$\begin{aligned} &\Sigma^{(2)}_{11} = (\lambda + 2\mu)\partial_1 U^{(2)}_1 + \lambda\partial_3 U^{(2)}_3, \quad \Sigma^{(2)}_{22} = \lambda(\partial_1 U^{(2)}_1 + \partial_3 U^{(2)}_3), \quad \Sigma^{(2)}_{12} = \mu\partial_1 U^{(2)}_2, \\ &\Sigma^{(2)}_{33} = \lambda\partial_1 U^{(2)}_1 + (\lambda + 2\mu)\partial_3 U^{(2)}_3, \quad \Sigma^{(2)}_{13} = \mu(\partial_3 U^{(2)}_1 + \partial_1 U^{(2)}_3), \quad \Sigma^{(2)}_{23} = \mu\partial_3 U^{(2)}_2. \end{aligned} \tag{2.3}$$

For the anisotropic coating layers, Hooke's law may be written as (using Voigt's abbreviated notation; Auld, 1990)

$$\begin{pmatrix} \Sigma_{11}^{(r)} \\ \Sigma_{22}^{(r)} \\ \Sigma_{33}^{(r)} \\ \Sigma_{23}^{(r)} \\ \Sigma_{13}^{(r)} \\ \Sigma_{12}^{(r)} \end{pmatrix} = \begin{pmatrix} C_{11} & C_{12} & C_{13} & 0 & 0 & C_{16} \\ C_{12} & C_{22} & C_{23} & 0 & 0 & C_{26} \\ C_{13} & C_{23} & C_{33} & 0 & 0 & C_{36} \\ 0 & 0 & 0 & C_{44} & C_{45} & 0 \\ 0 & 0 & 0 & C_{45} & C_{55} & 0 \\ C_{16} & C_{26} & C_{36} & 0 & 0 & C_{66} \end{pmatrix} \begin{pmatrix} \partial_1 U_1^{(r)} \\ 0 \\ \partial_3 U_3^{(r)} \\ \partial_3 U_2^{(r)} \\ \partial_3 U_1^{(r)} + \partial_1 U_3^{(r)} \\ \partial_1 U_2^{(r)} \end{pmatrix}, \quad r = 1, 3. \tag{2.4}$$

It should be noted here that if an orthotropic material is rotated about the x_3-axis (the normal to the plate), its stiffness matrix will be in the form shown in Eq. (2.4). This is the main reason for choosing monoclinic material symmetry in this paper. Finally, boundary and interface conditions must be supplied. Due to the symmetry of the configuration, the problem may be split into a symmetric and an antisymmetric case. The boundary conditions governing the symmetric subproblem are

$$\Sigma_{3j}^{(1)} = -F_j(\omega)\delta(x_1)/2, \quad x_3 = -a - h, \tag{2.5a}$$

$$\Sigma_{3j}^{(3)} = -F_j(\omega)\delta(x_1)/2, \quad x_3 = a + h, \tag{2.5b}$$

and the boundary conditions governing the antisymmetric subproblem are

$$\Sigma_{3j}^{(1)} = -F_j(\omega)\delta(x_1)/2, \quad x_3 = -a - h, \tag{2.6a}$$

$$\Sigma_{3j}^{(3)} = F_j(\omega)\delta(x_1)/2, \quad x_3 = a + h, \tag{2.6b}$$

where $\delta(x_1)$ is the Dirac delta "function". At the interfaces, continuity of the displacement and traction vectors must hold, i.e.,

$$U_j^{(1)} = U_j^{(2)}, \quad \Sigma_{3j}^{(1)} = \Sigma_{3j}^{(2)}, \quad x_3 = -a, \tag{2.7a}$$

$$U_j^{(2)} = U_j^{(3)}, \quad \Sigma_{3j}^{(2)} = \Sigma_{3j}^{(3)}, \quad x_3 = a. \tag{2.7b}$$

The solution to the original problem is obtained as the sum of the solutions to the symmetric and antisymmetric subproblems. After the problem is divided into a symmetric and antisymmetric subproblem, it is only necessary to consider half the structure. Since we are interested in the transient response on the top surface, $x_3 = -a - h$, only layers 1 and 2 are considered below.

3. The exact solution

In order to derive the exact solution to the wave propagation problem described in Section 2, the fields are spatially Fourier transformed in the x_1-direction as follows:

$$\widehat{U}(k) = \int_{-\infty}^{\infty} U(x_1) \mathrm{e}^{-\mathrm{i}kx_1} \, \mathrm{d}x_1, \Rightarrow U(x_1) = \frac{1}{2\pi} \int_{-\infty}^{\infty} \widehat{U}(k), \mathrm{e}^{\mathrm{i}kx_1} \, \mathrm{d}k. \tag{3.1}$$

The general solution in coating layer 1 may then be written as

$$\widehat{U}_j^{(1)} = \sum_{N=1}^{3} (A_N^+ V_{Nj}^+ \mathrm{e}^{\mathrm{i}k_{N3}^+(x_3+a+h)} + A_N^- V_{Nj}^- \mathrm{e}^{\mathrm{i}k_{N3}^-(x_3+a)}). \tag{3.2}$$

Six wave numbers k_{N3} and polarization vectors $(V_{Nj}, T_{Nj})^{\mathrm{T}}$ are obtained as the solutions to the eigenvalue problem

$$K\begin{pmatrix} \boldsymbol{V} \\ \boldsymbol{T} \end{pmatrix} = k_3 M\begin{pmatrix} \boldsymbol{V} \\ \boldsymbol{T} \end{pmatrix}, \tag{3.3}$$

which is obtained from Eqs. (2.2), (2.4), and (3.2). The wave numbers $k_{N3}^{\pm}$ and the corresponding polarization vectors $(V_{Nj}^{\pm}, T_{Nj}^{\pm})^{\mathrm{T}}$ are obtained from the six solutions by ordering them as $\mathrm{Im}k_{N3}^{+} \geqslant 0$ and $\mathrm{Im}k_{N3}^{-} \leqslant 0$. The traction vectors are obtained from the vectors $T_{Nj}^{\pm}$ and Eq. (3.2) as

$$\widehat{\Sigma}_{3j}^{(1)} = \sum_{N=1}^{3} (A_N^{+} T_{Nj}^{+} \mathrm{e}^{\mathrm{i}k_{N3}^{+}(x_3+a+h)} + A_N^{-} T_{Nj}^{-} \mathrm{e}^{\mathrm{i}k_{N3}^{-}(x_3+a)}). \tag{3.4}$$

The non-zero elements of the matrices K and M in Eq. (3.3) are

$$\begin{aligned}
&K_{13} = C_{55}k, \quad K_{14} = K_{25} = K_{36} = \mathrm{i}, \quad K_{23} = C_{45}k, \quad K_{31} = C_{13}k,\\
&K_{32} = C_{36}k, \quad K_{41} = C_{11}k^2 - \rho_{\mathrm{c}}\omega^2, \quad K_{42} = K_{51} = C_{16}k^2,\\
&K_{52} = C_{66}k^2 - \rho_{\mathrm{c}}\omega^2, \quad K_{63} = -\rho_{\mathrm{c}}\omega^2, \quad K_{64} = -\mathrm{i}k,\\
&M_{11} = -C_{55}, \quad M_{12} = M_{21} = -C_{45}, \quad M_{22} = -C_{44}, \quad M_{33} = -C_{33},\\
&M_{43} = -C_{13}k, \quad M_{44} = M_{55} = M_{66} = \mathrm{i}, \quad M_{53} = -C_{36}k.
\end{aligned} \tag{3.5}$$

The general solution in the isotropic plate is split into a symmetric and an antisymmetric part (Achenbach, 1973). The symmetric part is given by

$$\begin{aligned}
\widehat{U}_1^{(2)} &= \mathrm{i}kD_1 \cos(px_3) - qD_2 \cos(qx_3),\\
\widehat{U}_2^{(2)} &= \frac{k_s^2}{q} D_3 \cos(qx_3),\\
\widehat{U}_3^{(2)} &= -pD_1 \sin(px_3) + \mathrm{i}kD_2 \sin(qx_3),
\end{aligned} \tag{3.6}$$

and the antisymmetric part is given by

$$\begin{aligned}
\widehat{U}_1^{(2)} &= \mathrm{i}kD_4 \sin(px_3) + qD_5 \sin(qx_3),\\
\widehat{U}_2^{(2)} &= -\frac{k_s^2}{q} D_6 \sin(qx_3),\\
\widehat{U}_3^{(2)} &= pD_4 \cos(px_3) + \mathrm{i}kD_5 \cos(qx_3),
\end{aligned} \tag{3.7}$$

where $k_s = \omega\sqrt{\rho/\mu}$, $q = \sqrt{k_s^2 - k^2}$, $p = \sqrt{k_p^2 - k^2}$, and $k_p = \omega\sqrt{\rho/(\lambda + 2\mu)}$.

By applying the boundary and interface conditions Eqs. (2.5a), (2.5b), (2.7a) and (2.7b) and Eqs. (2.6a)–(2.7b), the integration constants in the symmetric and antisymmetric cases may be obtained, respectively. Note that we only need to apply the conditions at $x_3 = -a$ and $x_3 = -a - h$ due to the symmetry of the problem. Inversion of the spatial and temporal Fourier transforms finally give the exact solution to the wave propagation problem in the time domain.

4. An approximate solution

Since the coating layers are assumed to be thin relative to the wavelengths, approximating them in a simple fashion should be possible. An order h approximation used by Niklasson et al. (2000a) is employed here. Since the details on the approximation of the transient response due to a line force may be found elsewhere (Niklasson and Datta, submitted for publication), only a brief summary is given here.

The approximate boundary conditions state that (Niklasson et al., 2000a)

$$\Sigma_{3j}^{(2)} \mp h(A_{jm}U_m^{(2)} + B_{jm}\Sigma_{3m}^{(2)}) = -F_j\delta(x_1)/2, \quad x_3 = \pm a, \tag{4.1}$$

in the symmetric case, and

$$\Sigma_{3j}^{(2)} \mp h(A_{jm}U_m^{(2)} + B_{jm}\Sigma_{3m}^{(2)}) = \pm F_j\delta(x_1)/2, \quad x_3 = \pm a, \tag{4.2}$$

in the antisymmetric case. The non-zero elements of the matrices A_{jm} and B_{jm} are

$$\begin{aligned} &A_{11} = (C_{11} - C_{13}^2/C_{33})\partial_1^2 + \rho_c\omega^2, \quad A_{12} = A_{21} = (C_{16} - C_{13}C_{36}/C_{33})\partial_1^2, \\ &A_{22} = (C_{66} - C_{36}^2/C_{33})\partial_1^2 + \rho_c\omega^2, \quad A_{33} = \rho_c\omega^2, \\ &B_{13} = (C_{13}/C_{33})\partial_1, \quad B_{23} = (C_{36}/C_{33})\partial_1, \quad B_{31} = \partial_1. \end{aligned} \tag{4.3}$$

Since the thin coating layers have been replaced by the effective boundary conditions, a general solution is only needed in the isotropic plate. As in the previous section, a spatial Fourier transform is applied and the general solution is given by Eqs. (3.6) and (3.7). Approximating the thin layers thus result in significant simplifications. No general solutions are needed in the coating layers and the number of unknown integration constants is reduced from 18 to 6. Once again, only half the structure is considered and the boundary conditions Eqs. (4.1) and (4.2) at $x_3 = -a$ give the integration constants in the symmetric and antisymmetric cases, respectively. Inversion of the Fourier transforms finally gives the transient response in the isotropic plate. Since the field in the top coating layer is needed, a series expansion is used. The result is

$$U_j^{(1)}(x_1, x_3) \approx U_j^{(2)}(x_1, -a) + (x_3 + a)(\partial_3 U_j^{(2)}(x_1, x_3))_{x_3=-a}, \quad -a - h < x_3 < -a. \tag{4.4}$$

5. Numerical examples

In this section, numerical results are presented for a three-layered plate composed of a homogeneous isotropic core coated symmetrically on both sides with thin anisotropic layers. This example is chosen to illustrate the effect of anisotropy of the thin coating layers on the transient response of the plate. Especially, the effect of mode coupling due to the anisotropy is investigated. In addition, comparisons are made between the exact and approximate solutions. In all examples, the isotropic layer is made of nickel (Ni) with elastic properties $\lambda = 129.5$ GPa, $\mu = 84.7$ GPa, and density $\rho = 8910$ kg/m^3. The superconducting coating layers are made of the orthotropic superconductor YBCO having material properties given in Table 1 (Lei et al., 1993). Only the non-zero elastic constants relative to the crystal axes system are given in the table. In the examples below, propagation in different directions not coinciding with this system are shown and compared with the results for propagation along the symmetry axes. This is indicated by the angle between the x_1'-axis and x_1-axis, ϕ. The x_3- and x_3'-axes always coincide and ϕ is the rotation angle about the x_3-axis to get from the x_1'-axis to the x_1-axis. The transformation of the elastic constants from the crystal axes system $x_1'x_2'x_3'$ to the $x_1x_2x_3$-system is given by Auld (1990). The thickness of the isotropic plate is $2a = 100$ μm and the coating layers are each 5 μm thick ($h = 5$ μm).

In all examples, a force acting in the x_3-direction all along the x_2-axis is considered. The time dependence of the force is chosen to be (Pan and Datta, 1999; Niklasson and Datta, submitted for publication)

Table 1
Material properties of YBCO (C_{JM}' in GPa and ρ_c in kg/m^3)

C_{11}'	C_{22}'	C_{33}'	C_{44}'	C_{55}'	C_{66}'	C_{12}'	C_{13}'	C_{23}'	ρ_c
268	231	186	37	49	95	132	95	71	6333

$$f_j(t) = \sqrt{2/\pi}\delta_{j3} e^{-c_s^2(t-t_0)^2/8a^2} \sin(2\pi f_c t), \tag{5.1}$$

where $c_s^2 = \mu/\rho$, the time delay t_0 is 0.16 μs, and the center frequency f_c is varied. Figs. 2(a) and (b), show the line force $f_3(t)$ and the temporally transformed line force $F_3(\omega)$ for the center frequency $f_c = 32$ MHz.

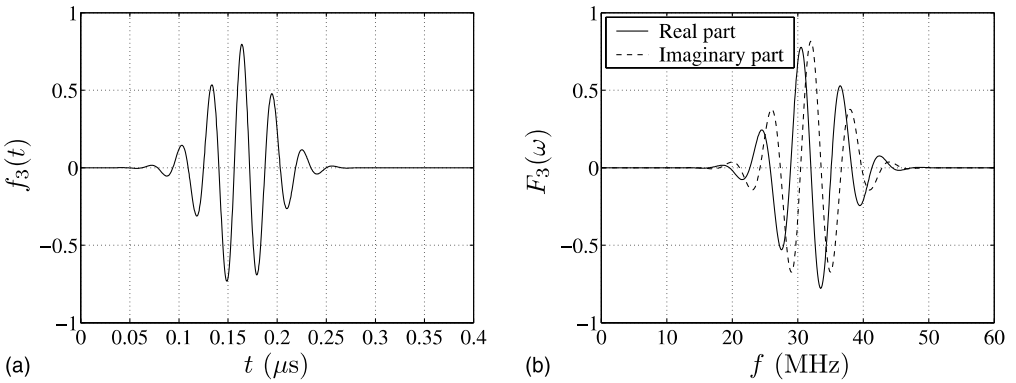

Fig. 2. The line force when $f_c = 32$ MHz in the (a) time and (b) frequency domains.

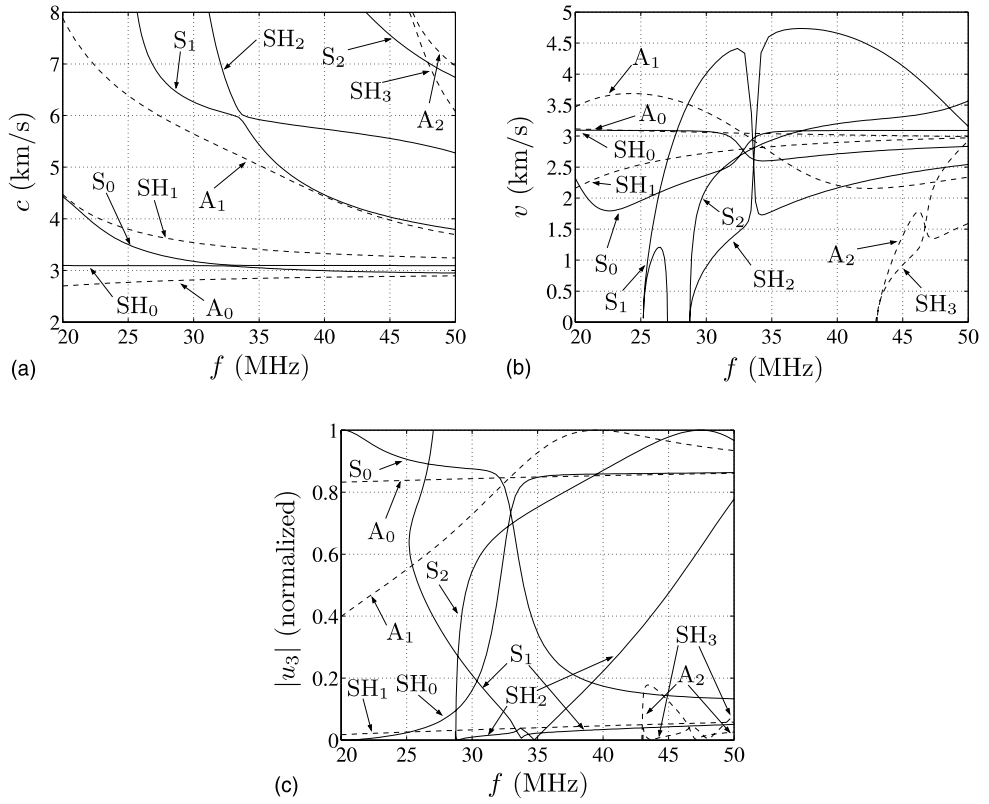

Fig. 3. (a) Phase velocity, (b) group velocity and (c) vertical displacement on the top surface for YBCO/Ni/YBCO, $\phi = 30°$. Solid lines are symmetric modes and dashed lines are antisymmetric modes.

As is seen in Fig. 2(b), the force is essentially zero outside an interval of width 30 MHz centered around f_c. In addition, only the x_3-component of the displacement field, u_3, is shown in the figures below. The main reason for the choices of direction of the line force and displacement component is that this is the most realistic situation from a experimental point of view. The observation point is located at $x_1 = \xi = 10$ mm, i.e., $u_3(\xi, -a-h, t)$ is shown. In order to show the effect of the layering, figures showing $u_3(\xi, -a-h, t)$ for a pure Ni plate of the same total thickness, i.e., 110 μm, are presented as well.

In Fig. 3(a), the dispersion curves for propagation in the direction $\phi = 30°$ is shown. Corresponding group velocities are shown in Fig. 3(b) and Fig. 3(c) shows the absolute value of the vertical displacement on the top surface of the plate associated with the different modes. Both symmetric and antisymmetric modes are depicted in these figures. These figures will be an aid to identifying the different signals by their arrival times and strengths. Fig. 3 clearly shows the coupling of the S_0 and SH_0 modes around 32 MHz, where a mode interchange takes place, as seen in Fig. 3(c) from the vertical displacements associated with these modes. The coupling of the S_1 and SH_2 modes at around 33 MHz is also clearly seen in this figure. The vertical displacements associated with them around this frequency are however quite small and are not expected to be measurable. In this study, attention was thus focused on the coupling between the S_0 and SH_0 modes for propagation directions different than 0° and 90°. This coupling due to anisotropy could be

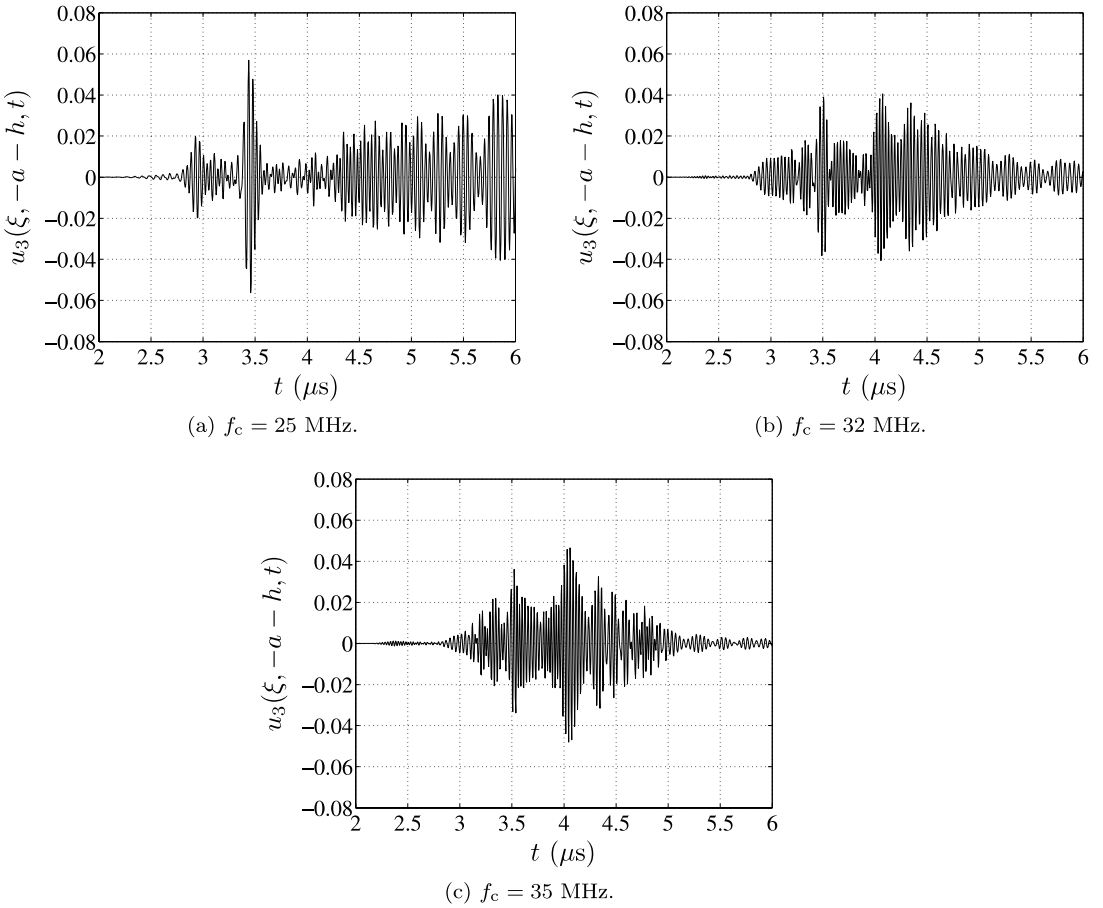

(a) $f_c = 25$ MHz.

(b) $f_c = 32$ MHz.

(c) $f_c = 35$ MHz.

Fig. 4. The vertical displacement on the top surface of a 110 μm thick Ni plate, 10 mm from the line force.

used to determine the in-plane anisotropic constants, C'_{12} and C'_{66}, of thin coating layers. It should be noted that when the propagation is not in directions of material symmetry, the modes are not purely extensional (S), flexural (A), or shear horizontal (SH) due to the mode coupling.

When the spatial and temporal Fourier transforms are inverted special care need be taken. Along the real k-axis a number of poles are located (zeros of the dispersion relation). Therefore, the integration contour is deformed into the complex k-plane. The contour used here is

$$k(s) = k_s s(1 - \mathrm{i}\alpha \mathrm{e}^{-\beta|s|}), \tag{5.2}$$

with $\alpha = 0.02$ and $\beta = 2$. In addition, symmetries of the integrands are used to reduce the integration interval to $0 \leqslant s < \infty$. After the deformation of the contour has been performed no singularities (poles) of the integrand exist anymore. The integrand is, however, still behaving badly. This is solved by employing the adaptive quadrature schemes by Xu and Mal (1985, 1987). When the approximate solution is computed, the tail of the integrand is computed by means of the exact solution since the approximation breaks down for large values of k. When the temporal Fourier transform is inverted, the exponential windowing technique is used (Pan and Datta, 1999). See Niklasson and Datta (submitted for publication) for more details on the numerical treatment.

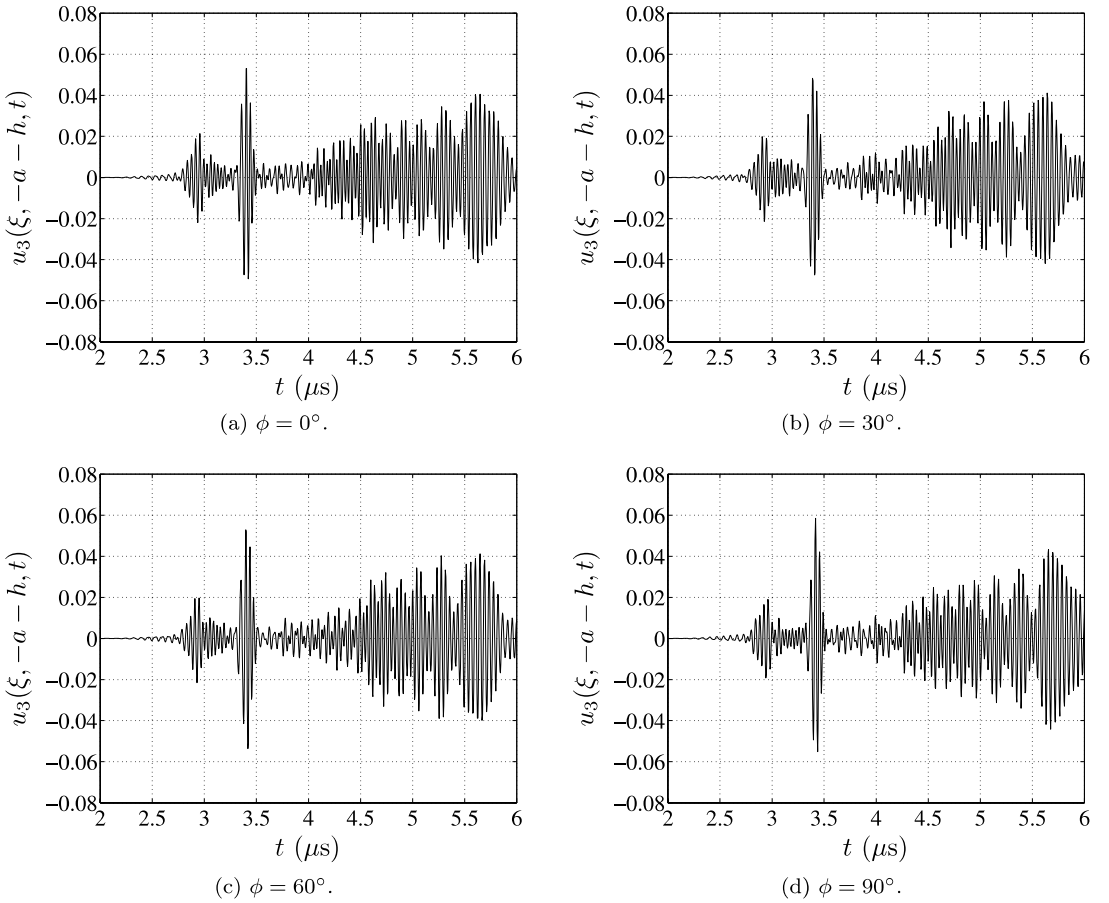

Fig. 5. The vertical displacement on the top surface of the YBCO/Ni/YBCO plate, 10 mm from a line force with $f_c = 25$ MHz.

For purposes of comparison between the homogeneous and coated plates, results for a 110 μm thick Ni plate are shown in Fig. 4 for three different values of the center frequency $f_c = 25$, 32, and 35 MHz. The vertical displacement on the top surface, $u_3(\xi, -a-h, t)$, is shown here. Fig. 4(a) clearly shows the arrival of the A_1 mode at 2.9 μs, followed by the arrival of the A_0 mode having a large amplitude. In Fig. 4(b), small amplitude S_1 mode appears first, followed by A_1, A_0, and then S_2 (3.9 μs) and S_0 (4.3 μs). The last has a large amplitude (comparable to A_0). The last two are seen to be prominent in Fig. 4(c) with arrival times earlier than in Fig. 4(b).

Turning now to the response of the coated plate, results for $\phi = 0°$, 30°, 60°, and 90° are shown in Fig. 5. The center frequency is 25 MHz. Comparison of Fig. 5 with Fig. 4(a) shows considerable similarity. The arrival times are a little sooner now. Note that in the cases when $\phi = 30°$ and 60°, the SH_0 and SH_1 modes are excited, but at this frequency their amplitudes are quite small. The strength of the A_0 mode is seen to be weakly influenced by the direction of propagation. Also, the signals arriving later are somewhat influenced by the anisotropy.

Fig. 6 shows the results for $f_c = 32$ MHz. This frequency is lower than that at which the interchange between the SH_0 and S_0 modes occur, but the former now has a significant vertical displacement component. It is found from Fig. 6 that the SH_0 mode arrives at the heels of the A_0 mode, which is followed by S_2

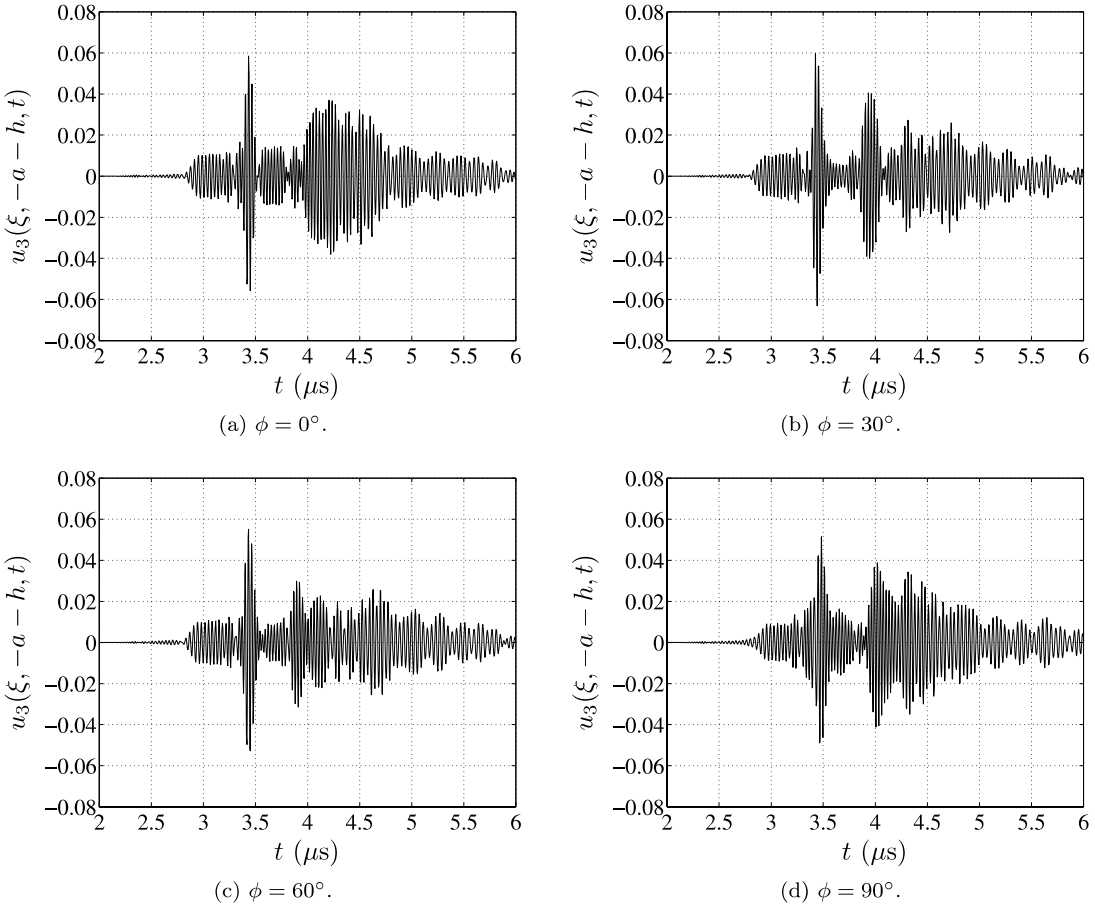

(a) $\phi = 0°$. (b) $\phi = 30°$.

(c) $\phi = 60°$. (d) $\phi = 90°$.

Fig. 6. The vertical displacement on the top surface of the YBCO/Ni/YBCO plate, 10 mm from a line force with $f_c = 32$ MHz.

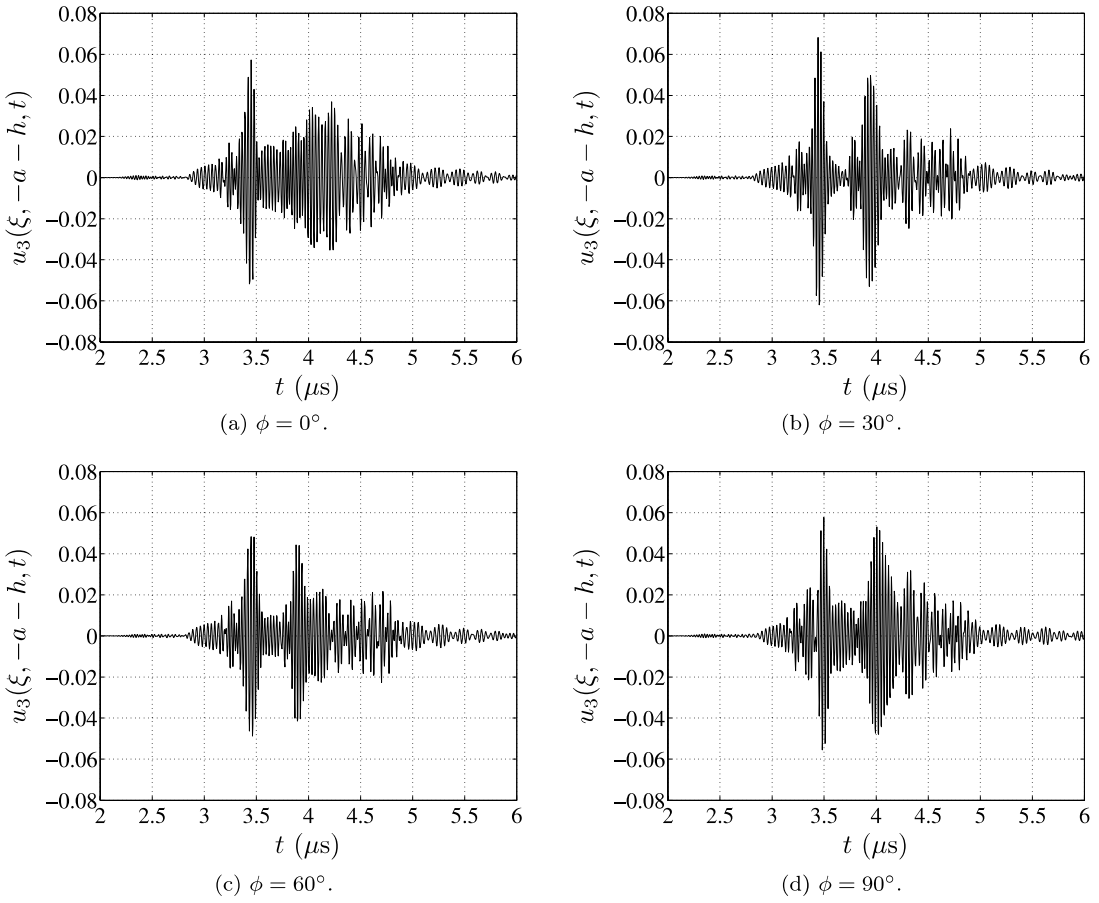

Fig. 7. The vertical displacement on the top surface of the YBCO/Ni/YBCO plate, 10 mm from a line force with $f_c = 35$ MHz.

and S_0 modes. There are two differences between this figure and Fig. 4(b). One difference is the layering and the other is the excitation of the SH_0 mode in Fig. 6(b) and (c).

As f_c is increased to 35 MHz, which is after the mode-interchange frequency, the signal is modified by the later arrival of the SH_0 mode with a large amplitude as well as the earlier arrival of the A_0 mode with a large amplitude. Note that S_0 mode with a small amplitude arrives almost at the same time as the A_0. Fig. 7 is significantly different than Fig. 6, which is at $f_c = 32$ MHz.

Figs. 8 and 9 show the results obtained using the $O(h)$ approximation for $f_c = 25$ and 32 MHz. Comparison of Figs. 5 and 8 show fairly good agreement. At the higher frequency, the results in Figs. 6 and 9 are quantitatively dissimilar, although there is qualitative agreement. The approximation seems to work quite well in predicting the primary features of the signals.

6. Concluding remarks

In this paper, the transient response of a three-layered superconducting tape due to a line force has been discussed. The tape consisted of an isotropic plate coated symmetrically with two thin superconducting

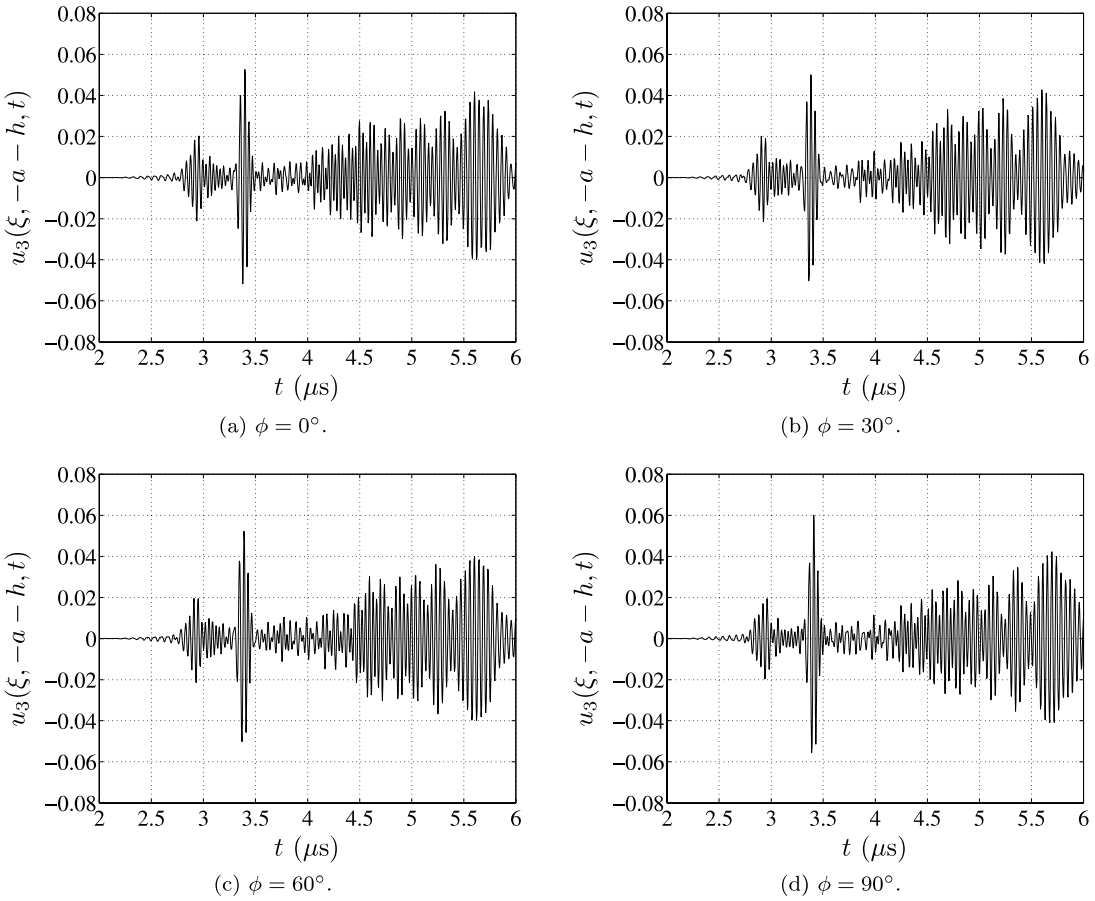

Fig. 8. The approximate vertical displacement on the top surface of the YBCO/Ni/YBCO plate, 10 mm from a line force with $f_c = 25$ MHz.

(anisotropic) layers. The main objective of this study was to investigate the possibility of measuring material properties of the thin coating layers at relatively low frequencies. Due to the anisotropy of the superconducting layers, the shear horizontal (SH) modes will be coupled with the extensional (S) and flexural (A) modes for off-symmetry-axis propagation. Especially the coupling of the first symmetrical (S_0) and first horizontal shear (SH_0) modes were of our interest since it occurs at a low frequency.

Numerical examples for a tape made of a Ni plate of thickness 100 μm coated with two identical YBCO layers, each of thickness 5 μm, have been presented. The mode interchange between the S_0 and SH_0 modes occurs at approximately 32 MHz for this specific configuration. In the examples, a line force normal to the top surface has been applied and the vertical response of the tape on the same surface as the line force has been studied. Due to the mode interchange, SH modes will be excited by this force for off-symmetry-axis propagation and may thus make it possible to measure in-plane elastic constants at relatively low frequencies. In order to capture the effects of the mode interchange, the frequency spectrum of the line force was of narrow band with a center frequency close to 32 MHz. For the lowest center frequency considered, 25 MHz, the effects of the anisotropy was small. Some effects of the anisotropy was seen in the first flexural mode (A_0). At the center frequency 32 MHz, which is slightly below the point of mode interchange between

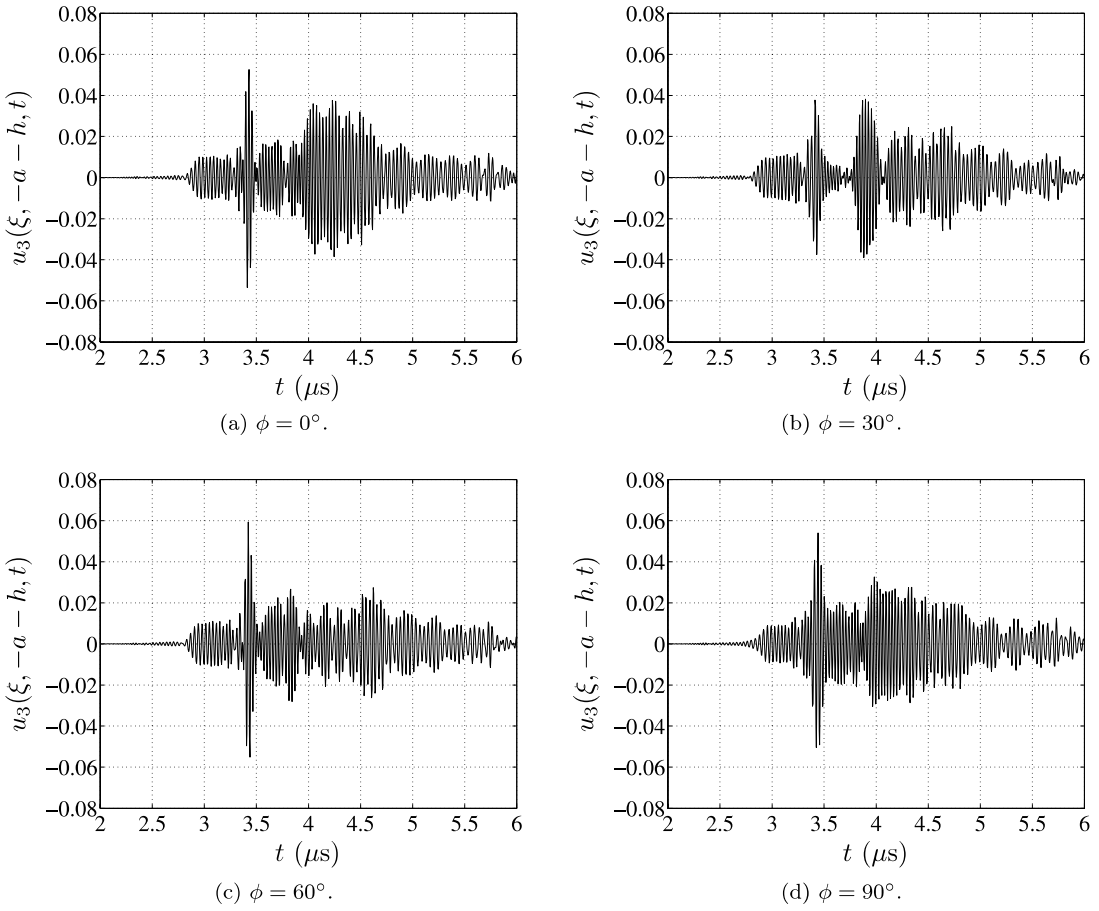

Fig. 9. The approximate vertical displacement on the top surface of the YBCO/Ni/YBCO plate, 10 mm from a line force with $f_c = 32$ MHz.

the S_0 and SH_0 modes, the anisotropy of the coating layers, was clearly seen. At this frequency, the S_0 and SH_0 modes are strongly coupled due to the anisotropy and both have strong vertical displacement components. At the highest center frequency, 35 MHz, the mode interchange has taken place and the character of the S_0 and SH_0 modes are now interchanged. Both modes still have strong vertical displacement components and the effect of anisotropy is clearly seen in this case as well. The conclusion is thus that the signal due to a narrow band excitation with a center frequency close to the interchange between the S_0 and SH_0 is fairly sensitive to the anisotropy even though the frequencies are relatively low.

Examples with a 110 μm homogeneous plate made of Ni was also presented in order to see the effect of the layering. As would be expected, the introduction of the coating layers significantly changes the transient response at the higher center frequencies (32 and 35 MHz). Most notable is that the amplitude of the first flexural mode A_0 was increased for the layered plate.

In addition to the exact solution, an approximation was computed. The approximation was based on replacing the thin coating layers by effective boundary conditions. From the numerical examples it was found that the approximation captures the features of the exact solution well qualitatively, but not very well quantitatively as the center frequency is increased.

Acknowledgements

The work of the first author (AJN) was made possible primarily through the financial assistance provided by the Swedish Foundation for International Cooperation in Research and Higher Education (STINT). The authors also gratefully acknowledge the support provided by the Department of Energy, Office of Basic Energy Sciences, Division of Materials Science and Engineering (DE-FG03-97ER14738).

References

Achenbach, J.D., 1973. Wave Propagation in Elastic Solids. North-Holland, Amsterdam.

Auld, B.A., 1990. Acoustic Fields and Waves in Solids, vol. 1. Krieger, FL.

Kim, J.O., Achenbach, J.D., Mirkarimi, P.B., Shinn, M., Barnett, S., 1992. Elastic constants of single-crystal transition-metal nitride films by line-focused acoustic microscopy. J. Appl. Phys. 72, 1805–1811.

Lei, M., Sarrao, J.L., Visscher, W.M., Bell, T.M., Thompson, J.D., Migliori, A., Welp, U.W., Veal, B.W., 1993. Elastic constants of a monocrystal of superconducting $YBa_2Cu_3O_{7-\delta}$. Phys. Rev. B 47, 6154–6156.

Levy, M. (Ed.), 1993. Physical Acoustics, vol. 20. Academic Press, New York.

Niklasson, A.J., Datta, S.K. Transient ultrasonic waves in multilayered superconducting plates. Report, Department of Mechanical Engineering, University of Colorado, Boulder, CO, accepted in ASME J. Appl. Mech.

Niklasson, A.J., Datta, S.K., Dunn, M.L., 2000a. On approximating guided waves in thin anisotropic coatings by means of effective boundary conditions. J. Acoust. Soc. Am. 108, 924–933.

Niklasson, A.J., Datta, S.K., Dunn, M.L., 2000b. On ultrasonic guided waves in a thin anisotropic layer lying between two isotropic layers. J. Acoust. Soc. Am. 108, 2005–2011.

Pan, E., Datta, S.K., 1999. Ultrasonic waves in multilayered superconducting plates. J. Appl. Phys. 86, 543–551.

Qu, J., Kundu, T. (Eds.), 2000. Nondestructive Evaluation and Characterization of Engineering Materials for Reliability and Durability Predictions AMD, vol. 240. The American Society of Mechanical Engineers, New York (also, NDE, vol. 18).

Shindo, Y., Ledbetter, H., Nozaki, H., 1995. Elastic constants and microcracks in $YBa_2Cu_3O_7$. J. Mater. Res. 10, 7–10.

Xu, P.-C., Mal, A.K., 1985. An adaptive integration scheme for irregularly oscillatory functions. Wave Motion 7, 235–243.

Xu, P.-C., Mal, A.K., 1987. Calculation of the inplane Green's functions for a layered viscoelastic solid. Bull. Seismol. Soc. Am. 77, 1823–1837.